buildings

MDPI

Article

Developing a Practical Thermal Performance Index for Radiant Terminals—Structural Thermal Resistance

Xiang Zhou [1], Dandan Wang [1], Yunliang Liu [1], Maohui Luo [1,*], Seyed Mohammad Hooshmand [2] and Andreas Wagner [2]

[1] School of Mechanical Engineering, Tongji University, Shanghai 201804, China; zhouxiang@tongji.edu.cn (X.Z.); 2232755@tongji.edu.cn (D.W.); liuyunliang2020@163.com (Y.L.)
[2] Department of Architecture, Karlsruhe Institute of Technology, 76131 Karlsruhe, Germany; seyed.hooshmand@kit.edu (S.M.H.); andreas.wagner2@kit.edu (A.W.)
* Correspondence: luomaohui@tongji.edu.cn

Abstract: Radiant terminals have been widely applied in heating and cooling systems. However, few existing thermal performance evaluation indices can reflect the influence of structural forms on heat transfer performance. This study introduces the structural thermal resistance (R_s) to rapidly evaluate the structure form's effects. First, theoretical analysis and experimental tests were introduced. Three types of terminals, including the copper conduit graphite plate (CCGP), plastic tube-embedded metal plate (PTMP), and capillary network-embedded structural plate (CNSP) were tested in the laboratory. Then, the CNSP terminals were taken as validation examples. The results show that the R_s values of the same type of radiant terminal tend to be stable and constant. The variations in R_s within the same type of radiant terminals were small both under cooling and heating conditions. Only when the terminal structure changed, the R_s would change. This suggests that the R_s can reflect the complex heat transfer processes inside the radiant terminals while distinguishing different terminal types. The validation analysis showed an average relative error of 3.4% and 2.9% for cooling and heating, respectively. Lastly, the potential application of R_s in practical applications was discussed, and a Python-based online tool was developed to help design, operate, and evaluate radiant terminals.

Keywords: radiant air conditioning; structural thermal resistance; radiant terminals; radiant heat transfer

Citation: Zhou, X.; Wang, D.; Liu, Y.; Luo, M.; Hooshmand, S.M.; Wagner, A. Developing a Practical Thermal Performance Index for Radiant Terminals—Structural Thermal Resistance. *Buildings* **2023**, *13*, 2938. https://doi.org/10.3390/buildings13122938

Academic Editor: Constantinos A. Balaras

Received: 28 October 2023
Revised: 19 November 2023
Accepted: 22 November 2023
Published: 24 November 2023

1. Introduction

Radiant air conditioning systems mainly exchange heat in the form of radiation. The application of radiant air conditioning system has been increasing in recent years, covering various building types such as residences, hospitals, and airport terminals [1,2]. Compared with convection air conditioning, radiant heating and cooling shows energy-saving potential [3,4] and better indoor thermal comfort [5,6]. Tantiwichien et al. [7] found that a radiant cooling system can save 41% of cooling energy compared to split air conditioner. Yau and Hasbi [8] compared two green office buildings using radiant cooling and a traditional cooling system in Malaysia. Their results show that the two radiant systems can meet indoor thermal comfort and air quality requirements and standards [9,10].

Radiant air conditioning systems which use water as the medium mainly include two parts of heat transfer processes. One is the heat transfer from the water to the radiant surface of the terminal, which is mainly through convection and conduction. The other is the heat transfer from the radiant surface to the indoor air and other surfaces, which is mainly through convection and radiation approaches.

When studying the heat transfer between the circulating water and the radiant surface of the terminal, Fonseca Diaz et al. [11] treated the radiant ceiling as a fin and established an internal thermal resistance model. The heat transfers between the internal structures were considered separately and the heat loss along the opposite surface (the surface opposite to the radiant surface) was estimated. However, applying this method to analyze the

internal heat transfer process is very cumbersome. Once the pipe embedding method or the internal structure change, it needs to be re-modeled and re-calculated. Liu et al. [12] revised the composite fin model and the equivalent thermal resistance model to improve the model accuracy and expand their application range, but the calculation is more complex. To simplify the calculations, Li et al. [13] equivalented the heat transfer process between the layers of the radiant plate as a series of thermal resistance models, and calculated the equivalent thermal resistance according to the physical and geometric parameters of the plate.

Many studies have also investigated heat transfer between the radiant surface and the indoor environment, where the heat transfer coefficient indices were widely adopted. Khalifa and Marshall [14] compared the heat transfer coefficient differences in different locations of the room. Awbi and Hatton [15] calculated the natural convective heat transfer coefficient and radiant heat transfer capacity by measuring indoor air temperature and surface temperature. Causone et al. [16] determined the reference temperatures for calculating the radiant heat transfer coefficient, natural convection heat transfer coefficient, and integrated heat transfer coefficient. They also obtained the reference values of these three coefficients under cooling and heating conditions. Andres-Chicote et al. [17] compared the calculated heat transfer coefficient reference values, and suggested that the operating temperature can be obtained by combining a variety of indoor air temperatures and wall temperatures. Zheng et al. [18] investigated the effects of different parameters on the heat transfer performance of radiant floor systems under the influence of solar radiation and analyzed the heat transfer process in the room after the addition of solar radiation by establishing an R-C model. Wang et al. [19] established the simplified numerical models for calculating the heat transfer and surface temperature of prefabricated floor or ceiling terminals. The heat transfer models were validated by using the radiant plate surface temperature. Based on this, a calculation tool for four prefabricated floor or ceiling terminals was developed. Ren et al. [20] developed an online tool to calculate the asymmetric and the mean radiant temperatures in a typical office room with radiant terminals.

From the above studies, we found that the structural form of radiant terminals is a key factor that affects the heat transfer performance, which will then directly affect the design of radiant systems, and appropriate indices that can reflect the heat transfer performance are of particular importance. From this aspect, the existing research still has some shortcomings. First, the specific structure inside the radiant terminal must be clarified and complex heat transfer models must be established before conducting any calculation. Once the radiant terminal changes, the model needs to be re-established. Second, detailed size and physical parameters of each structure must be elaborated because they will change the temperature distribution, which makes the calculation more complicated.

The heat transfer capacity and surface temperature are the widely used thermal performance indices currently [21]. However, the heat transfer capacity can only reflect the heat transfer ability at specific water supply temperature and indoor temperature, lacking in universal significance for different temperature combinations. The surface temperature is mainly used to describe the risk of condensation and may easily be affected by environmental conditions. Both indices may vary with terminal types due to the change in structure.

This study introduces the structural thermal resistance (R_s). This index ignores the complex heat exchange process inside the radiant terminal and treats it as a whole.To examine whether the R_s can be used as a universal design tool for radiant air conditioning, three types of terminals were tested first; then, the CNSP terminals were taken as validation examples, and lastly the copper conduit metal plate (CCMP) was taken as an application example. After testing and verifying the new index, an online tool was developed to make it more convenient for the calculation and application of R_s.

2. Methods

2.1. Heat Transfer Model of Radiant Terminals

The R_s was used to describe the steady state heat transfer processes. To simplify the heat transfer model at the radiant terminal, the following assumptions were made: (1) The three-dimensional heat transfer at the terminal is simplified into two-dimensional heat transfer (see Figure 1), which means that the heat transfer perpendicular to the paper direction is not considered. (2) Use a single node to describe the indoor room temperature, which means that the room temperature is considered uniform. (3) All the cooling or heat supplied by the water is transferred downward to the room node without considering the upward heat transfer to the ceiling. This is because, in engineering practice (see Figure 1), an insulation layer is usually installed on the opposite surface of the radiant surface to reduce heat transfer to the opposite direction.

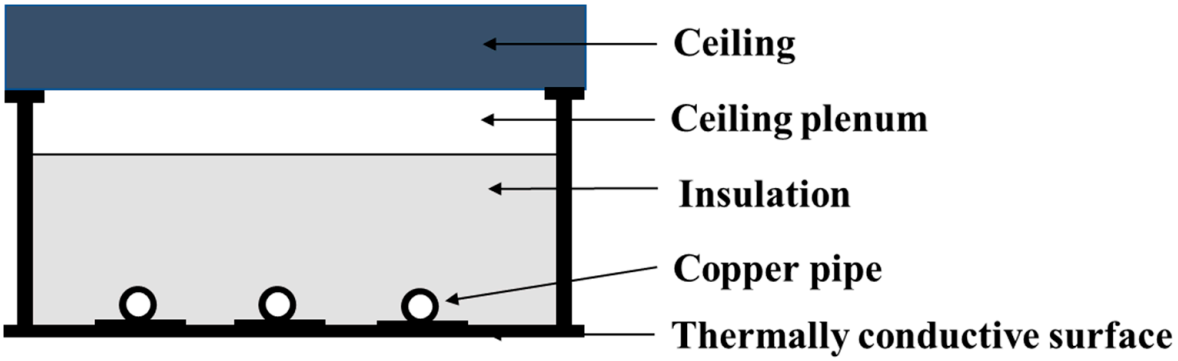

Figure 1. Schematic diagram of a typical radiant panel.

The heat transfer between the radiant terminal surface and the room can be divided into two parts. One is natural convection with room air. The other is radiant heat transfer with other room surfaces. These two parts can be described by using the natural convective heat transfer coefficient and the radiant heat transfer coefficient (see Figure 2a). On this basis, the model can be further simplified by using an integrated heat transfer coefficient to represent the comprehensive effect of radiation and convection, as shown in Figure 2b. The reference temperatures corresponding to these three heat transfer coefficient values are based on the recommendation of Causone et al. [16]. The indoor air temperature (T_a), the average unloaded surface temperature ($AUST$), and the indoor room temperature (T_o) are employed as the reference temperatures for natural convective heat transfer coefficient (h_c), radiant heat transfer coefficient (h_r), and integrated heat transfer coefficient (h_t), respectively. $T_{w,avg}$ is the average temperature of water supply and return in °C. T_s is the average indoor-side surface temperature of the radiant plate in °C. T_a is the indoor air temperature in °C. $AUST$ is the average uncooled/unheated surface temperature in °C. T_o is the indoor room temperature in °C which indicates the combined effect of T_a and $AUST$(see Equation (9)). R_c and R_r are the natural convective heat transfer resistance and radiant heat transfer resistance, where $R_c = 1/h_c$, $R_r = 1/h_r$, (m^2·K)/W. R_t is the integrated heat transfer resistance, where $R_t = 1/h_t$, (m^2·K)/W. When establishing the heat transfer model between the circulating water and the radiant surface, a node of average temperature of supply and return water was assumed at the location of the pipeline in radiant plates.

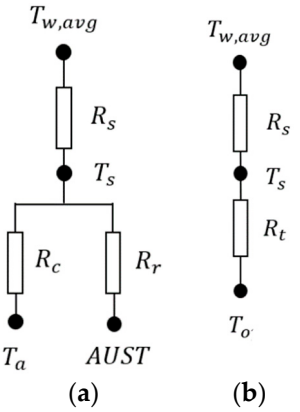

Figure 2. Simplified heat transfer models of the radiant terminal. (**a**) Simplified model that considers the indoor convection and radiation separately. (**b**) Simplified model that considers the indoor convection and radiation comprehensively.

2.2. Testing on Radiant Terminals

2.2.1. Experimental Facility

Four typical radiant plates were selected in this study, shown in Figure 3. (1) The copper conduit graphite plate (CCGP, Figure 3a). (2) The plastic tube-embedded metal plate (PTMP, Figure 3b). (3) The capillary network-embedded structural plate (CNSP, Figure 3c). (4) The copper conduit metal plate (CCMP, Figure 3d). Among them, the first three radiant terminals (CCGP, PTMP, and CNSP) were tested under cooling and heating conditions while the CCMP serves as an application case in the Discussion Section. The heat transfer areas of CCGP, PTMP, and CNSP are 12.48 m^2, 11.72 m^2, and 12 m^2, respectively. For these three radiant terminals, 7 sets of experiments were carried out under cooling and heating conditions. Under heating conditions, the air temperature in the room was 20 °C, and the water supply temperatures were 34, 35, 36, 37, 38, 39, and 40 °C, respectively. Under cooling conditions, the air temperature in the room was 26 °C, and the water supply temperatures were 14, 15, 16, 17, 18, 19, and 20 °C, respectively.

2.2.2. Experimental Apparatus

The experiments were carried out in a climatic chamber with a dimension of 4.2 m (length) × 3.6 m (width) × 2.5 m (height). The chamber included two rooms, of which the inner room was the indoor environment installed with radiant ceiling panel. A total of 12 dummies were arranged symmetrically along the longest centerline in the chamber to simulate indoor heat sources. The external room was installed with fan coil to control the wall temperature. A simplified schematic about the chamber is shown in Figure 4a, where the green and red lines indicate the supply and return water, respectively. Figure 4b,c represent a schematic and test scene of the internal arrangement of the chamber, respectively. The emissivity of all the wall surfaces of the chamber was 0.9 to ensure that the indoor emissivity met the requirements of EN-14240 [22]. The combination method of internal and external heat sources was adopted [21,22]. The dummies with incandescent bulbs were used as the indoor heat source in the cooling test conditions while fan coils cooling in the interlayer was used as the outdoor cooling source in the heating test conditions.

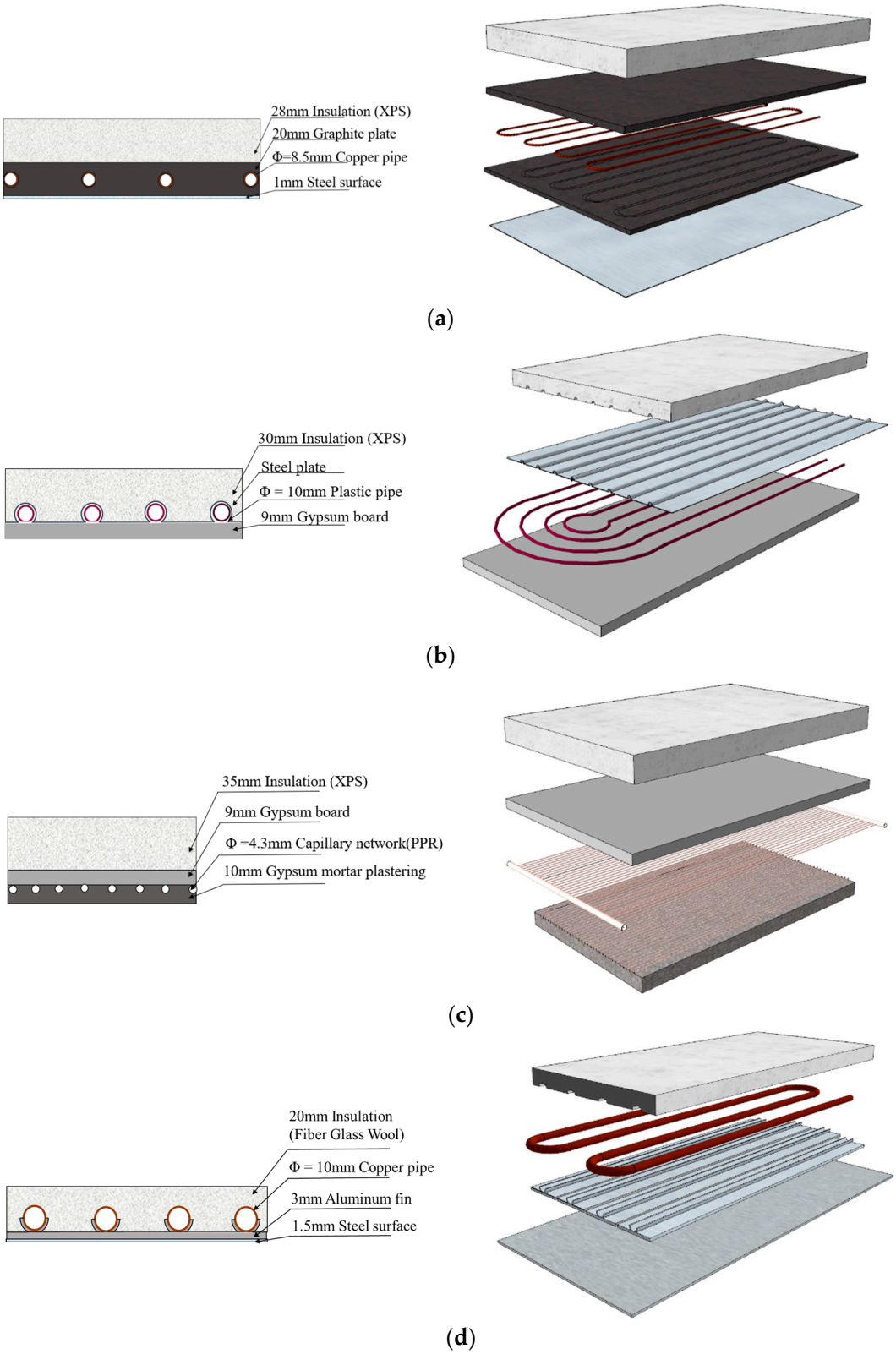

Figure 3. Structures of radiant terminals in this study. (**a**) Copper conduit graphite plate. (**b**) Plastic tube-embedded metal plate. (**c**) Capillary network-embedded structural plate. (**d**) Copper conduit metal plate.

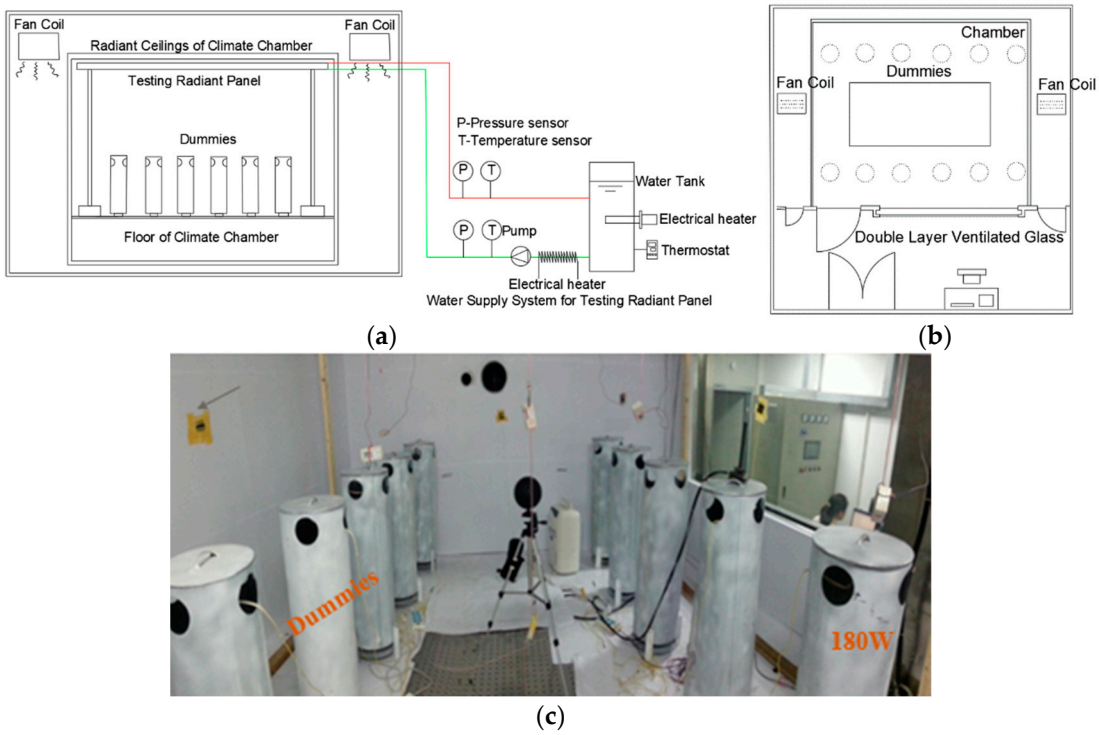

Figure 4. Arrangement of the climate chamber; (**a**) simplified schematic about the chamber; (**b**,**c**) a schematic and test scene of the internal arrangement of the chamber.

2.2.3. Test Protocol

The heat transfer performance of radiant ceilings with different water supply temperatures was studied under cooling and heating conditions separately. The air temperature in the internal room was 26 °C as the cooling condition and seven water supply temperatures were 14, 15, 16, 17, 18, 19, and 20 °C, respectively. The air temperature in the internal room was 20 °C as the heating condition and seven water supply temperatures were 34, 35, 36, 37, 38, 39, and 40 °C, respectively. During the test, the indoor air temperature (T_a) was maintained within ±0.5 °C and the relative humidity (RH) was maintained within ±5%. The test parameters include water supply ($T_{w,s}$) and return temperatures ($T_{w,r}$), water flow rate (m_w), air temperature (T_a), and average radiant surface temperature of the plate (T_s). The electric heating and measurement points were arranged according to EN14240 standard [22].

The specific experimental steps are as follows:

1. Turn on the indoor air conditioning system and wall water supply system. Adjust the indoor air temperature, relative humidity, and wall temperature to the set temperature.
2. Turn off the air supply of the air conditioning system to keep the indoor temperature stable with the fan coils in the interlayer operating. Turn on the test block water supply system and set the thermostat of the constant-temperature water tank. The water tank was equipped with a platinum resistance temperature sensor to monitor the water temperature in the tank. A line-shape electric heater was installed on the water supply pipe to adjust the water temperature precisely.
3. Turn on the electric dummies to maintain the room temperature at the set temperature (cooling conditions). Turn on the fan coils in the interlayer to maintain the room temperature at the set temperature (heating conditions).
4. When all the parameters reach a stable state, the temperatures, flow rate, and pressure of the water supply and return were recorded. Based on these measurements, the radiant terminal's heat transfer capacity and R_s can be calculated.

2.3. Calculating the R_s

As shown in Figure 2, for steady-state heat transfer, the heat transfer capacity of the radiant terminals can be expressed as the heat absorption/release of water, which is shown in Equation (1).

$$q = \frac{c_w m_w |T_{w,r} - T_{w,s}|}{A_s} \quad (1)$$

where q is the radiant terminal heat transfer capacity, W/m^2; c_w is the specific heat of water, J/(kg·K); m_w is the water flow rate, kg/s; $T_{w,s}$, $T_{w,r}$ are the supply and return water temperatures, °C; A_s is the radiant heat transfer area, m^2.

The total heat flux density through the radiant panel can also be expressed as the sum of the radiant heat transfer and natural convection heat transfer.

$$q = q_c + q_r = h_c|T_a - T_s| + h_r|AUST - T_S| \quad (2)$$

where q_c, q_r indicate the heat transfer in the form of natural convection and radiation, respectively, W/m^2; h_c, h_r are natural convection heat transfer coefficient and radiant heat transfer coefficient, respectively, W/(m^2·K); T_s is the average indoor-side surface temperature of the radiant plate in °C; T_a is the air temperature in °C; $AUST$ is the average uncooled/unheated surface temperature as the reference temperature for the calculation of the radiant heat transfer coefficient in °C, which can be calculated by Equation (4) for radiant heat transfer [13] or Equation (3) for convection heat transfer.

$$AUST = \frac{\sum_{j=1}^{n} A_j T_j}{\sum_{j=1}^{n} A_j} \quad (3)$$

or

$$AUST = \left[\sum_{j=1}^{n} \left(F_{s-j} T_j^4\right)\right]^{0.25} \quad (4)$$

where T_j is the j$_{th}$ surface average temperature in °C; A_j is the j$_{th}$ surface area in m^2; F_{s-j} is the angular coefficient between the surface of the radiant panel and the j$_{th}$ room surface.

Radiant heat transfer capacity indicates the heat exchanged between the radiant panel and the indoor environment through radiation, and the calculation method refers to the ASHRAE standard [23].

$$q_r = 5 \times 10^{-8}\left(T_s^4 - AUST^4\right) \quad (5)$$

Natural convection heat transfer capacity represents the heat exchanged between the radiant ceiling and the indoor environment through natural convection, which can be expressed as Equation (6).

$$q_c = q - q_r \quad (6)$$

The reference temperature of radiant heat transfer coefficient is the average uncooled/unheated surface temperature ($AUST$), as shown in Equation (7).

$$h_r = \frac{q_r}{|T_s - AUST|} \quad (7)$$

The reference temperature of natural convective heat transfer coefficient is the indoor air temperature (T_a), which can be expressed as Equation (8).

$$h_c = \frac{q_c}{|T_s - T_a|} \quad (8)$$

The heat transfer model between the surface of the radiant ceiling and the indoor environment can be further simplified by considering the comprehensive effect of the radiation heat transfer and the natural convective heat transfer, and it can be expressed by the integrated heat transfer coefficient. Since the radiant heat transfer coefficient and the natural convective heat transfer coefficient follow different laws, the integrated heat transfer coefficient cannot simply be expressed as the sum of the two, so the indoor room

temperature should be used as its reference temperature. Its calculation method can be expressed as follows:

$$T_o = \frac{h_c T_a + h_r AUST}{h_c + h_r} \tag{9}$$

$$h_t = \frac{q}{|T_s - T_o|} \tag{10}$$

The heat transfer equation from the radiant ceiling surface to the indoor environment can be expressed as thermal resistance perspective as well. Equations (11)–(13) show the radiant heat transfer resistance (R_r), the natural convective heat transfer resistance (R_c), and the integrated heat transfer resistance (R_t) expressions.

$$R_r = \frac{1}{h_r} \tag{11}$$

$$R_c = \frac{1}{h_c} \tag{12}$$

$$R_t = \frac{1}{h_t} \tag{13}$$

The heat transfer from the circulating water to the radiant panel surface can be expressed by Equation (14).

$$q = \frac{|T_{w,avg} - T_s|}{R_s} \tag{14}$$

Therefore, the R_s can be expressed as Equation (15).

$$R_s = \frac{|T_s - T_{w,avg}|}{q} \tag{15}$$

2.4. Validating the $\boldsymbol{R_s}$

To verify the reliability of the R_s, we took the CNSP (Figure 3c) as an example. Cross-validating experiments with different indoor temperatures and supply-water temperatures under cooling and heating conditions was conducted. For cooling conditions, the indoor air temperatures were set up as 24, 26, 28, 30, and 32 °C while the supply-water temperatures were set up as 14, 15, 16, 17, 18, 19, and 20 °C. For the heating conditions, the indoor temperatures were set up as 16, 18, 20, 22, and 24 °C while the supply-water temperatures were set up as 34, 35, 36, 37, 38, 39, and 40 °C. Other details of the validating experiments were consistent with the experiments described in Section 2.2. The validation is based on the reference values of the integrated heat transfer coefficient and R_s of the CNSP. The heat transfer capacity of the radiant plate was calculated by using the R_s, and then it was compared with the heat absorption/release of the circulating water measured through the experiments. The specific derivation is as follows.

According to the simplified heat transfer model (see Figure 2), the heat transfer capacity can be expressed as Equation (16).

$$q = \frac{\left|T_s - \frac{(T_{w,r} + T_{w,s})}{2}\right|}{R_s} \tag{16}$$

In this way, the heat transfer capacity can be expressed by the heat transfer from the radiant surface to the indoor environment.

$$q = \frac{|T_o - T_s|}{\frac{1}{h_t}} \tag{17}$$

Meanwhile, the heat transfer capacity can also be expressed by heat absorption/release of the circulating water.

$$q = \frac{c_w m_w |T_{w,r} - T_{w,s}|}{A_s} \tag{18}$$

Combining the Equations (16)–(18), the return-water temperature, heat transfer capacity, and the average indoor-side surface temperature of the radiant plate can be expressed as Equations (19) and (20), respectively.

$$q = \frac{c_w m_w \left| \frac{T_o + \left(\frac{c_w m_w \left(R_s + \frac{1}{h_t} \right)}{A_s} - \frac{1}{2} \right) T_{w,s}}{\frac{c_w m_w \left(R_s + \frac{1}{h_t} \right)}{A_s} + \frac{1}{2}} - T_{w,s} \right|}{A_s} \tag{19}$$

$$T_s = T_o - \frac{q}{h_t} \tag{20}$$

where q determined by Equation (19) is the heat transfer capacity based on the R_s. The reliability of the R_s can be analyzed by comparing the q values with the heat absorption/release of the circulating water that was measured via experiments.

3. Results

3.1. Heat Transfer Coefficient of the Radiant Terminals

According to previous research [16], the h_r, h_c, h_t of radiant terminals with different types at different temperatures can be approximated as constant when there is no forced convection under stable working conditions. When considering the heat transfer between the radiant surface and the room, these three parameters were analyzed. Figures 5–7 show the changes in these three coefficients for three types of radiant terminals.

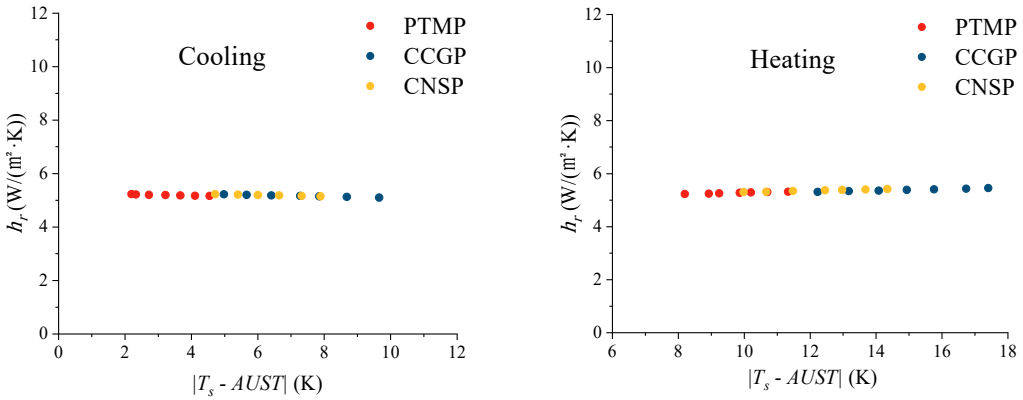

Figure 5. Experimental values of radiant heat transfer coefficient.

Figure 5 shows that, with the change in temperature difference between the radiant surface and the room, the radiant heat transfer coefficient of different types of radiant terminals can be regarded as a constant value. Once the radiant system was fixed, the angular coefficient and the emissivity of the surfaces in the room remained unchanged. According to Equations (5) and (7), changing the indoor surface temperature within a reasonable range will not significantly affect the radiant heat transfer coefficient.

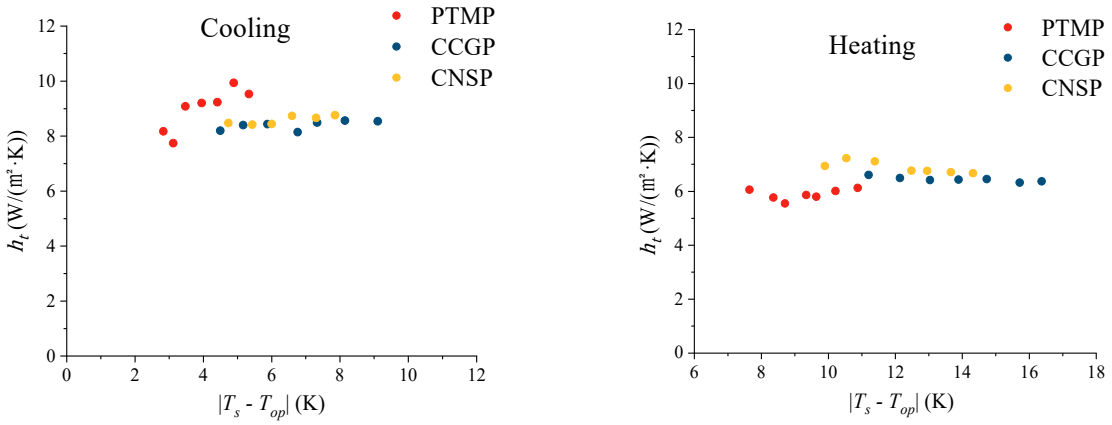

Figure 6. Experimental values of natural convective heat transfer coefficient.

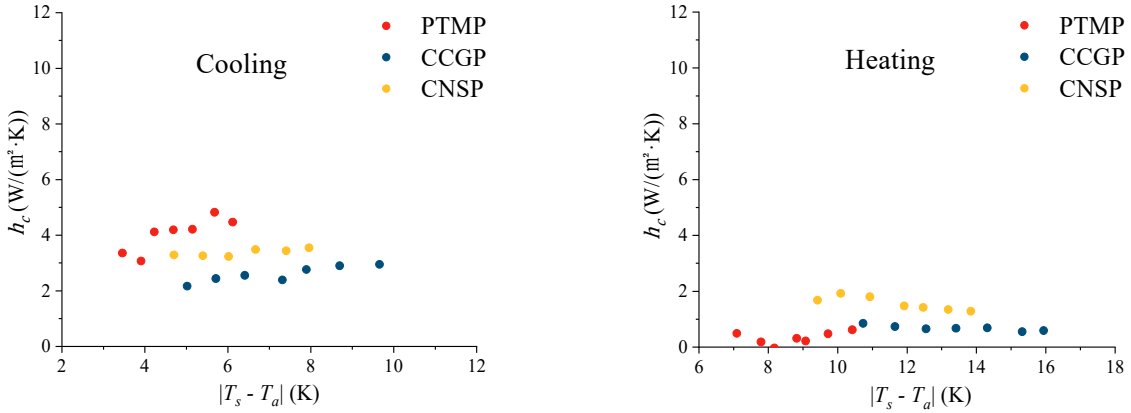

Figure 7. Experimental values of integrated heat transfer coefficient.

For the same type of radiant terminal, the natural convection heat transfer coefficient under the cooling condition is significantly greater than that under the heating condition, which is because the buoyancy force caused by the vertical temperature difference in the room makes the air movement under cooling more intense. Therefore, the natural convection during cooling tends to be stronger under the same temperature difference. Higher water supply temperatures need to be used if the indoor air temperature is to reach the experimental setting of 20 °C under heating conditions, which leads to higher T_s, and therefore the temperature difference during heating is significantly higher than that during cooling. Under the same cooling or heating conditions, changing the temperature difference, the natural convective heat transfer coefficient tends to be stable while there exist slight differences between different terminals. These variances may be due to different types of materials or other reasons that need to be further confirmed.

The integrated heat transfer coefficient considers the comprehensive effects of convection and radiation. Since the radiant heat transfer coefficient is stable, the variances in the integrated heat transfer coefficient follow the same pattern with the natural convection heat transfer coefficient. For the same type of radiant terminal, the integrated heat transfer coefficient under the cooling condition is significantly greater than that under the heating condition. Under the same cooling or heating condition, with the change in temperature difference, the integrated heat transfer coefficient of the same type of radiant ceiling was stable.

Table 1 summarizes the reference values of these three radiant terminals in existing studies. For the radiant heat transfer coefficient, the results in this study are very close to previous research results. It is recommended to select 5.3 W/(m^2·K) as the reference value. Under the same cooling or heating condition, the natural convective heat transfer coefficients of different types of radiant terminals are slightly different but the variance is

small, which can be considered as stable. It is recommended to choose 3.3 W/(m^2·K) and 0.9 W/(m^2·K) as reference values for cooling and heating, respectively. Although the value of 0.9 W/(m^2·K) may have a large deviation, it has little impact on the overall heat transfer due to its low weighting factor in the total heat transfer under the heating condition. For the integrated heat transfer coefficient, it is recommended to select 8.7 W/(m^2·K) under cooling conditions and 6.4 W/(m^2·K) under heating conditions.

Table 1. Summarize of heat transfer coefficients for the radiant surfaces.

	Natural Convection Heat Transfer Coefficient h_c W/(m^2·K)		**Radiant Heat Transfer Coefficient h_r W/(m^2·K)**	**Integrated Heat Transfer Coefficient h_t W/(m^2·K)**	
	cooling	heating		cooling	heating
Causone et al. [16]	4.4	0.3	5.6	13.2	5.8
Khalifa et al. [14]	3.1–3.6	0.5	5.5		
Min et al. [24]	3.6–4.8	0.1–0.3			
Andres-Chicot et al. [17]	4.2		5.4	8.5	
Awbi et al. [15]	2.8–3.9				
Present study	3.3	0.9	5.3	8.7	6.4

3.2. R_s of the Radiant Terminals

Figure 8 shows the calculated R_s values of the three tested radiant terminals under cooling and heating conditions. The fluctuation in R_s of the same radiant terminal is relatively small and can be approximated as a constant value. Comparing the cooling and heating conditions, once the type of radiant terminal was determined, the changes in R_s were small. However, the R_s values of different types of radiant terminals varied significantly. For example, the R_s values of PTMP are 0.096 (m^2·K)/W under cooling conditions and 0.116 (m^2·K)/W under heating conditions, while those of CCGP are 0.007 (m^2·K)/W under cooling conditions and 0.0119 (m^2·K)/W under heating conditions.

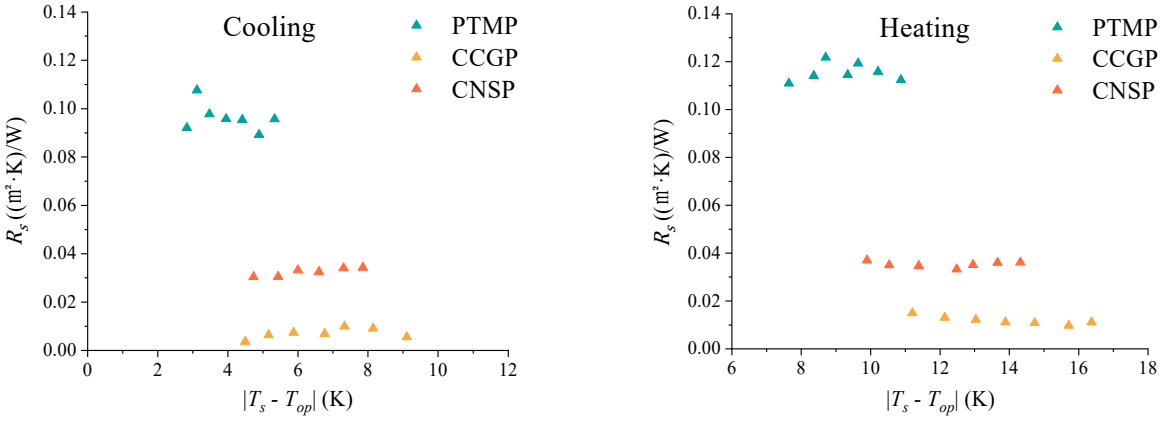

Figure 8. Thermal resistance value of the radiant terminal structure.

The R_s values of the same radiant terminal tended to be stable with the changes in the external environment once the cooling or heating conditions were determined. The R_s values mainly corelated with the terminal's structural forms and materials. This suggests that the concept of R_s can be employed as an effective index to reflect its structural characteristics and the corresonding influences on the terminal's heat transfer performance. This observation is a good response to our original intention to introduce the R_s, that is, using this index to simplify and reflect the complex heat transfer process caused by the structural forms of different radiant terminals, and to analyze the heat transfer performance of the radiant terminals.

For the three tested radiant terminals, their average R_s values under different working conditions have been summarized in Table 2. Taking the CNSP terminal as an example,

its average R_s values are 0.033 (m^2·K)/W under cooling conditions and 0.035 (m^2·K)/W under heating conditions.

Table 2. Structure thermal resistance of radiant terminals.

Radiant Type	Cooling Conditions (m^2·K)/W			Heating Conditions (m^2·K)/W		
	Fluctuation Range	**Mean Value**	**Standard Deviation**	**Fluctuation Range**	**Mean Value**	**Standard Deviation**
PTMP	(89.2–107.6) × 10^{-3}	0.096	0.0058	(110.9–121.8) × 10^{-3}	0.116	0.0038
CCGP	(3.7–10.0) × 10^{-3}	0.007	0.0021	(9.7–15.0) × 10^{-3}	0.0119	0.0017
CNSP	(30.4–34.3) × 10^{-3}	0.033	0.0017	(33.3–37) × 10^{-3}	0.035	0.0012

3.3. Validation of the R_s

After identifying the R_s of a radiant terminal, its heat transfer capacity under different combinations of indoor temperature and water supply temperature can be calculated by Equation (19). The heat transfer capacity values calculated by the validating conditions were compared with the heat absorption/release of the circulating water obtained from the experimental measurements. Figure 9 and Table 3 show the results.

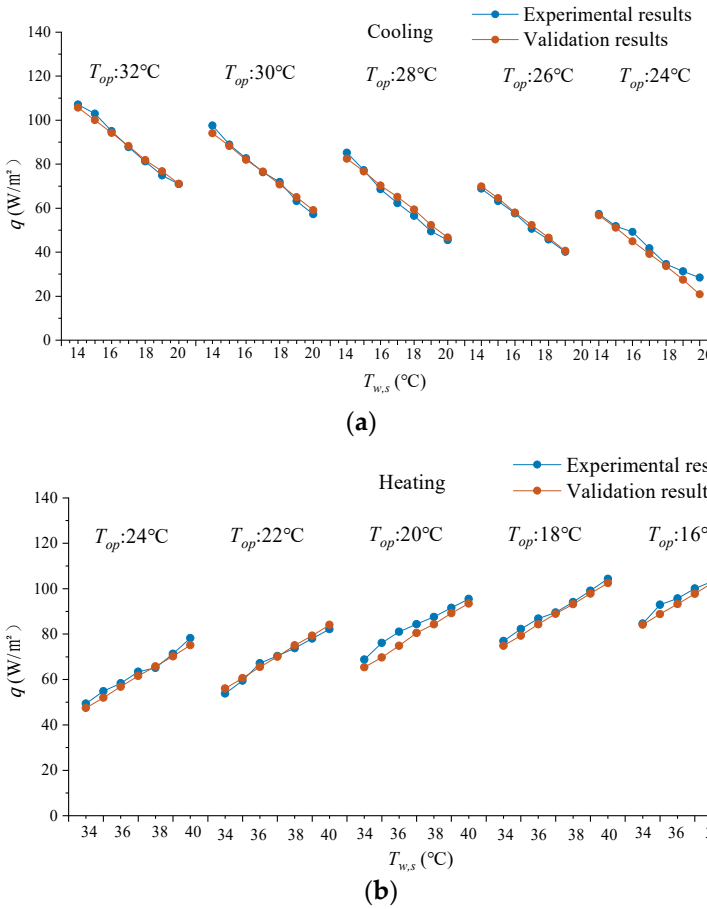

Figure 9. Comparison of experiment results and validation results.

Table 3. Relative error of the validation.

Cooling	T_{op}	32 °C	30 °C	28 °C	26 °C	24 °C
	Relative error	1.3%	1.9%	3.5%	1.7%	8.4%
Heating	T_{op}	24 °C	22 °C	20 °C	18 °C	16 °C
	Relative error	3.0%	2.1%	4.9%	2.0%	2.5%

The average relative error between the calculated and measured heat transfer capacity values were within 3.4% and 2.9% for cooling and heating, respectively. The higher error (8.4%) at T_{op} 24 °C was partially due to the reduced temperature difference and reduced heat transfer. Also, there may be random errors in the actual measurement process. This result supports the conclusion that it is reliable to use the R_s to reflect the complex heat transfer processes at the radiant terminals, and to describe the heat transfer performance of different radiant plates.

4. Discussion

Compared with existing studies, this study simplified the heat transfer model by using the R_s. By doing this, the complex heat transfer process inside the radiant terminal can be ignored and considered as a whole, which leads to a universal applicability for different terminals. Based on the above observations, the potential application case and possible limitations of the R_s are discussed as follows.

4.1. Potential Application of the $\boldsymbol{R_s}$

From the above results, the R_s can be used as a representative parameter to reflect the heat transfer capacity of different radiant terminals. Considering the variety of radiant terminals, the R_s values can be determined first and then used to analyze the terminal's heat transfer performance. Based on Figure 2, the following steps can be applied to make engineering estimates.

(1) Determine the R_s of a radiant terminal with two methods. One is experimental test. The experiments should be carried out under cooling or heating conditions. According to the simplified R_s model, the R_s values can be calculated according to Formula (21) by measuring the indoor room temperature T_o, average water supply and return temperature $T_{w,avg}$, and heat transfer capacity q. The other is through the heat transfer performance curve (normally, radiant terminal products should have this curve) to deduce its R_s. For example, if the $q-\left|T_{w,avg}-T_o\right|$ curve of the radiant terminal has already been known, performing a linear regression to obtain a result like $q=a_1\left|T_{w,avg}-T_o\right|+b_1,\ R_1^2=c_1$ ($a_1,\ b_1,\ c_1$ here are constant), the R_s of its radiant terminal can be deduced by Equation (21). If the $q-\left|T_{w,avg}-T_s\right|$ curve of the radiant terminal has already been known, performing a linear regression to obtain a result like $q=a_2\left|T_{w,avg}-T_o\right|+b_2,\ R_2^2=c_2$, ($a_2,\ b_2,\ c_2$ here are constant), the R_s of its radiant terminal can be deduced by Equation (22).

$$R_s=\frac{\left|T_{w,avg}-T_o\right|}{q}-\frac{1}{h_t} \tag{21}$$

$$R_s=\frac{\left|T_{w,avg}-T_s\right|}{q} \tag{22}$$

Taking the $q-\left|T_{w,avg}-T_o\right|$ curve (shown in Figure 10) (The green squares represent the measured data points, and the red line represents the result of fitted curve based on the actual data) of a certain radiant terminal under cooling conditions as an example, a regression equation $y=6.7898x+4.8808$, $R^2=0.9869$ can be fitted, so that a R_s value of about 0.02 ($m^2\cdot K$)/W can be obtained from Equation (21).

(2) The R_s obtained by step (1) can be applied for calculating the heat transfer performance of radiant terminals. The design parameters include heat transfer conditions, interior design temperature, water supply temperature, area of radiant roof, and water flow rate. According to the Formulas (19) and (20), the heat transfer capacity and the average temperature of the radiant surface can be calculated. To this end, whether there is a risk of condensation can better be estimated.

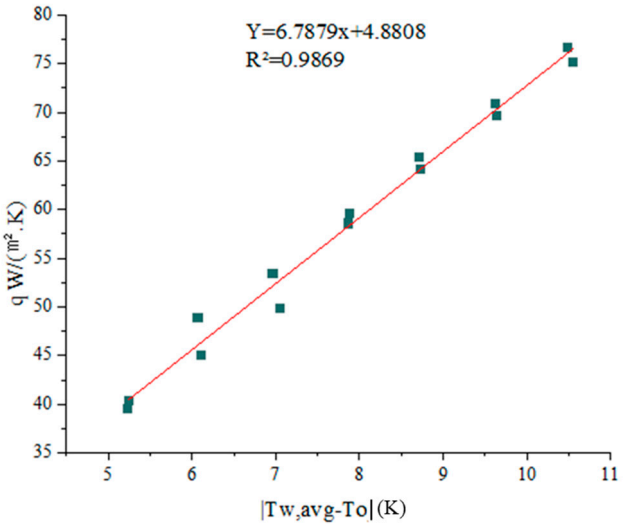

Figure 10. Heat transfer performance curve of a certain radiant terminal.

To demonstrate the above steps, we take another common radiant terminal, the copper conduit metal plate (CCMP, Figure 3d), as an example. Its R_s can be obtained through experimental measurement on T_o, $T_{w,avg}$, and q under different conditions. The tested R_s values are 0.012 (m^2·K)/W under cooling conditions and 0.006 (m^2· K)/W under heating conditions. The comparisons with the other three types of radiant terminals have been shown in Figure A1 in Appendix A.

After obtaining the value of the R_s, it can help to obtain a more intuitive relationship between the heat transfer capacity and the room temperature and the water supply temperature. Taking the CCMP as an example, the results are shown in Figure A2 in Appendix A.

For the CCMP, if the water supply temperature is 14 °C, the water flow rate is 0.24 m^3/h, the radiant plate heat transfer area is 11 m^2, and the indoor room temperature is 26 °C, and it can be calculated using Equations (19) and (20) that the heat transfer capacity should be 81.9 W/m^2 and that the inner surface temperature of the radiant plate should be 16.6 °C.

4.2. Online Tool Development and Application Example

To make the application of the R_s calculation more convenient, a Python-based online tool was developed based on the above derivation processes (http://en.tongji-rac.com/, accessed on 27 October 2023). This tool can help the design and operation of radiant terminals. The first module is the calculation of R_s. On this module, an Excel template (see Appendix B) can be downloaded. Then, the R_s values of the radiant terminal under heating and cooling conditions will be returned after entering all the data into the Excel template. Appendix C explains how to fill the template table. At the same time, the Excel template will calculate the average indoor-side surface temperature of the radiant plate based on the data entered by the user automatically, which will be used to meet the needs of the calibration. The second module is the calculation of heat transfer performance. It can invoke the R_s of the radiant terminal obtained by the first module and return the dew point temperature under different humidity according to the indoor design temperature, the return water temperature, the average temperature of the radiant plate surface, and the heat transfer capacity of the terminal.

Taking the CCMP terminal mentioned in Section 4.1 as an example, the input parameters were attached as Appendix D. Table 4 and Figure 11 show the calculated results.

Table 4. Case of online tool.

The first module	Input	Water supply temperature ($T_{w,s}$)	Water return temperature ($T_{w,r}$)	Average unloaded surface temperature ($AUST$)	Indoor air temperature (T_a)	Heat transfer capacity (q)
	Output	R_s under cooling conditions 0.012 (m^2·K)/W		R_s under heating conditions 0.006 (m^2·K)/W		
The second module	Input	Heat transfer conditions Cooling	Indoor room temperature (T_o) 26 °C	Water supply temperature ($T_{w,s}$) 14 °C	Radiant heat transfer area (A_s) 11 m^2	Water flow rate (m_w) 0.24 m^3/h
	Output	Integrated heat transfer coefficient (h_t) 8.7 W/(m^2·K)	Water return temperature ($T_{w,r}$) 17.2 °C	Inner surface temperature of the radiant plate (T_s) 16.6 °C		Heat transfer capacity (q) 81.9 W/m^2

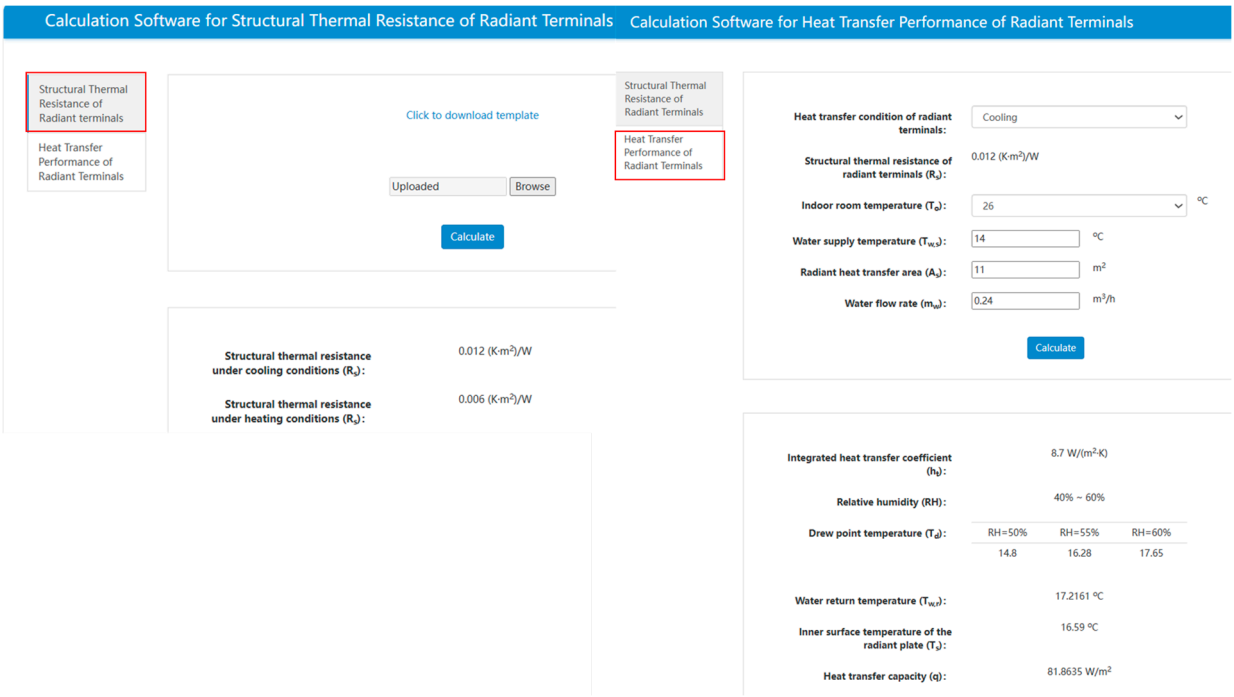

Figure 11. Online tool demonstration.

4.3. Limitations and Uncertainty Analysis of this Study

First, the supply and return water temperatures of radiant terminals were used to calculate the heat transfer capacity so that the heat transfer from the radiant panels to the space outside of the laboratory was not taken into account. For a target room (the room with the radiant ceiling), both the upper and lower rooms have radiant air conditioning, and the error of calculation due to the reverse heat transfer was ignored. For the case wherein the upper and lower rooms do not have air conditioning on if the Sun is shining directly on the top surface of the room, the error due to the reverse heat transfer needs to be modified. Second, in the case of large temperature differences between supply and return water, the linear average of temperatures may be inappropriate due to the nonlinearities in radiant heat transfer with temperature.

5. Conclusions

In this study, the concept of R_s is introduced to reflect the influence of structure forms on radiant terminals' heat transfer performance. Three typical radiant terminals were tested under variant conditions to calculate and validate the R_s values. The results suggest that this new concept of R_s has universal significance for different types of radiant terminals under both heating and cooling conditions. The R_s values of the CCGP, PTMP,

and CNSP were 0.007 ($m^2 \cdot$ K)/W, 0.096 ($m^2 \cdot$ K)/W, and 0.033 ($m^2 \cdot$ K)/W under cooling and 0.0119 ($m^2 \cdot$ K)/W, 0.116 ($m^2 \cdot$ K)/W, and 0.035 ($m^2 \cdot$ K)/W under heating, respectively. The validation tests on the CNSP showed an error of 2.9% and 3.4% for heating and cooling, respectively, which can meet the requirements for practical engineering applications.

The index of R_s can simplify the complicated heat transfer analysis at radiant terminals while reflecting the influence of form structures. By using the R_s, some critical indices of radiant terminals' heat transfer performance can be quantitatively and accurately calculated. These indices include but are not limited to the integrated heat transfer coefficient, heat transfer capacity, radiant surface temperature, and return water temperature.

To help the practical application of R_s, a Python-based online tool was developed. This tool can help to conveniently calculate R_s values and other key heat transfer performance indices with limited input information and guided processes. This can expand R_s application in practical engineering.

Author Contributions: Methodology, X.Z. and D.W.; Software, D.W. and Y.L.; Resources, X.Z. and M.L.; Data curation, D.W. and Y.L.; Writing—original draft, D.W.; Writing—review & editing, M.L., S.M.H. and A.W.; Funding acquisition, X.Z. and M.L. All authors have read and agreed to the published version of the manuscript.

Funding: The research was supported by the China National Key R&D Program during the 14th Five-year Plan Period (No. 2022YFC3801500), the National Natural Science Foundation of China (No. 52178087), the Fundamental Research Funds for the Central Universities (No. 2022-4-YB-06), the National Engineering Research Center of New Energy Vehicles and Power Systems, Shanghai Key Lab of Vehicle Aerodynamics and Vehicle Thermal Management Systems, and the German research foundation (DFG, No. WA 1155/7-1).

Data Availability Statement: The data used in this study were obtained from the results of sample testing provided by different radiant panel manufacturers, and we are not able to provide specific test data due to the confidentiality requirements of the manufacturers.

Conflicts of Interest: The authors declare no conflict of interest.

Nomenclature

A_j	The jth surface area, m^2
A_s	Radiant heat transfer area, m^2
$AUST$	Average unloaded surface temperature, °C
CCGP	Copper conduit graphite plate
CCMP	Copper conduit metal plate
CNSP	Capillary network-embedded structural plate
c_w	Specific heat of water, J/(kg·K)
F_{s-j}	Angular coefficient between the surface of the radiant panel and the jth room surface
h_c	Natural convective heat transfer coefficient, W/(m^2·K)
h_r	Radiant heat transfer coefficient, W/(m^2·K)
h_t	Integrated heat transfer coefficient, W/(m^2·K)
m_w	Water flow rate, kg/s
PTMP	Plastic tube-embedded metal plate
q	Heat transfer capacity, W
q_c	Heat transfer in the form of natural convection, W
q_r	Heat transfer in the form of radiation, W
RH	Relative humidity
R_c	Natural convective heat transfer resistance, (m^2·K)/W
R_r	Radiant heat transfer resistance, (m^2·K)/W
R_t	Integrated heat transfer resistance, (m^2·K)/W
R_s	Structural thermal resistance of the terminal, (m^2·K)/W
T_a	Indoor air temperature, °C
T_j	jth surface average temperature, °C
T_o	Indoor room temperature, °C

T_s	Average indoor-side surface temperature of the radiant plate, °C
$T_{w,avg}$	Average temperature of water supply and return, °C
$T_{w,r}$	Water return temperature, °C
$T_{w,s}$	Water supply temperature, °C

Appendix A

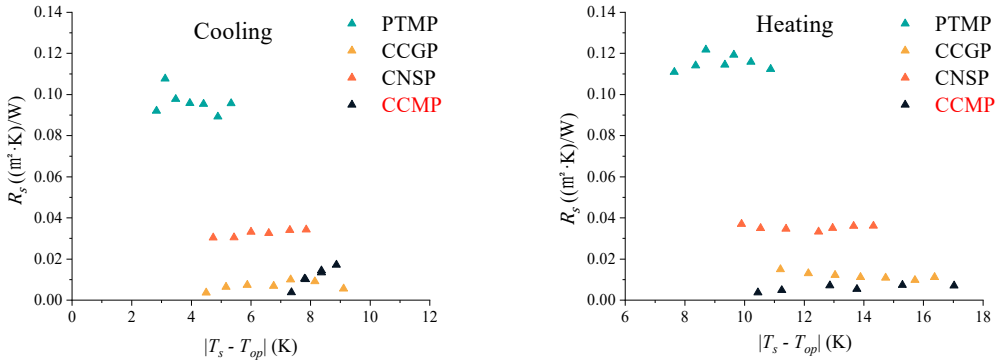

Figure A1. Values of R_s including the type of copper conduit metal plate.

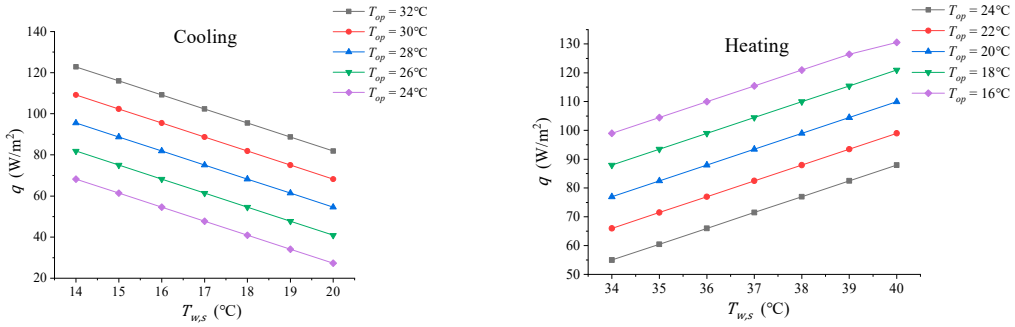

Figure A2. Heat transfer capacity of the CCMP.

Appendix B

When using the Excel template in the first module of the online tool, the data entered should include: water supply temperature ($T_{w,s}$), water return temperature ($T_{w,r}$), average unloaded surface temperature ($AUST$), indoor air terperature (T_a), and heat transfer capacity (q).

Cooling					
Water supply temperature $T_{w,s}$ (℃)	Water return temperature $T_{w,r}$ (℃)	Average unloaded surface temperature $AUST$ (℃)	Indoor air temperature T_a (℃)	Heat transfer capacity q (W/m²)	Average indoor-side surface temperature of the radiant plate Ts (℃)
					0
					0
					0
					0
					0
					0
Heating					
Water supply temperature $T_{w,s}$ (℃)	Water return temperature $T_{w,r}$ (℃)	Average unloaded surface temperature $AUST$ (℃)	Indoor air temperature T_a (℃)	Heat transfer capacity q (W/m²)	Average indoor-side surface temperature of the radiant plate Ts (℃)
					0
					0
					0
					0
					0
					0

Figure A3. Excel template for download of online tool.

Appendix C

When entering data, please enter these five sets of data at the same time. If you lack average unloaded surface temperature ($AUST$) or indoor air temperature (T_a), you can complete another set of data according to $AUST = T_a$, which meets the accuracy requirements in engineering applications.

Please note: up to 300 sets of data are automatically calculated in this template, if you have more experimental data, please directly drop down and fill.

Appendix D

The input case for the Excel template is shown in Figure A4.

Cooling					
Water supply temperature $T_{w,s}$ (℃)	Water return temperature $T_{w,r}$ (℃)	Average unloaded surface temperature *AUST* (℃)	Indoor air temperature T_a (℃)	Heat transfer capacity q (W/m^2)	Average indoor-side surface temperature of the radiant plate *Ts* (℃)
14.25	17.07	25	25	72.77	16.53837209
15.18	17.81	25	25	67.87	17.10813953
16.16	18.64	25	25	64	17.55813953
14.31	17.3	26	26	77.16	17.02790698
15.18	18	26	26	72.77	17.53837209
16.16	18.8	26	26	68.13	18.07790698
Heating					
Water supply temperature $T_{w,s}$ (℃)	Water return temperature $T_{w,r}$ (℃)	Average unloaded surface temperature *AUST* (℃)	Indoor air temperature T_a (℃)	Heat transfer capacity q (W/m^2)	Average indoor-side surface temperature of the radiant plate *Ts* (℃)
32	29.4	20	20	66.89	30.4515625
35	31.8	20	20	82	32.8125
40	35.6	20	20	108.98	37.028125
35	32.2	22	22	72	33.25
38	34.48	22	22	88.1	35.765625
40	36.03	22	22	97.88	37.29375

Figure A4. Case of filling out the Excel template.

References

1. Hu, R.; Niu, J. A review of the application of radiant cooling & heating systems in Mainland China. *Energy Build.* **2012**, *52*, 11–19.
2. Moreira, M.; Silva, T.; Dias-De-Oliveira, J.; Neto, F.; Amaral, C. Numerical modelling of radiant systems and phase change materials in building applications—A review. *Appl. Therm. Eng.* **2023**, *234*, 121342. [CrossRef]
3. Ren, J.; Zhu, L.; Wang, Y.; Wang, C.; Xiong, W. Very low temperature radiant heating/cooling indoor end system for efficient use of renewable energies. *Sol. Energy* **2010**, *84*, 1072–1083. [CrossRef]
4. Dhamodharan, P.; Ayalur, B.K.; Judefelix, J.; Prabakaran, R.; Kim, S.C. Energy saving potential in radiant cooling system by utilizing air-conditioning condensate: A strategy for green building rating. *Appl. Therm. Eng.* **2023**, *236*, 121492. [CrossRef]
5. Tian, Z.; Love, J.A. A field study of occupant thermal comfort and thermal environments with radiant slab cooling. *J. Affect. Disord.* **2008**, *43*, 1658–1670. [CrossRef]
6. Gao, S.; Li, Y.; Wang, Y.; Meng, X.; Zhang, L.; Yang, C.; Jin, L. A human thermal balance based evaluation of thermal comfort subject to radiant cooling system and sedentary status. *Appl. Therm. Eng.* **2017**, *122*, 461–472. [CrossRef]
7. Tantiwichien, A.-U. An Experimental and Simulated Study on Thermal Comfort. *Int. J. Eng. Technol.* **2013**, *5*, 177–180. [CrossRef]
8. Yau, Y.H.; Hasbi, S. Field analysis of indoor air quality in high rise and low rise green offices with radiant slab cooling systems in Malaysia. *Indoor Built Environ.* **2013**, *24*, 174–184. [CrossRef]
9. *MS 1525:2007*; Malaysian Standard: Code of Practice on Energy Efficiency and Renewable Energy for Non-Residential Building. Department of Standards Malaysia: Kuala Lumpur, Malaysia, 2007.
10. *55:2010*; Thermal Environmental Conditions for Human Occupancy. ASHRAE: Peachtree Corners, GA, USA, 2010.
11. Diaz, N.F.; Lebrun, J.; André, P. Experimental study and modeling of cooling ceiling systems using steady-state analysis. *Int. J. Refrig.* **2010**, *33*, 793–805. [CrossRef]
12. Liu, Y.; Wang, D.; Liu, J. Study on heat transfer process for in-slab heating floor. *Build. Environ.* **2012**, *54*, 77–85. [CrossRef]
13. Li, Q.-Q.; Chen, C.; Zhang, Y.; Lin, J.; Ling, H.-S. Simplified thermal calculation method for floor structure in radiant floor cooling system. *Energy Build.* **2014**, *74*, 182–190. [CrossRef]
14. Khalifa, A.; Marshall, R. Validation of heat transfer coefficients on interior building surfaces using a real-sized indoor test cell. *Int. J. Heat Mass Transf.* **1990**, *33*, 2219–2236. [CrossRef]
15. Awbi, H.; Hatton, A. Natural convection from heated room surfaces. *Energy Build.* **1999**, *30*, 233–244. [CrossRef]
16. Causone, F.; Corgnati, S.P.; Filippi, M.; Olesen, B.W. Experimental evaluation of heat transfer coefficients between radiant ceiling and room. *Energy Build.* **2009**, *41*, 622–628. [CrossRef]
17. Andrés-Chicote, M.; Tejero-González, A.; Velasco-Gómez, E.; Rey-Martínez, F.J. Experimental study on the cooling capacity of a radiant cooled ceiling system. *Energy Build.* **2012**, *54*, 207–214. [CrossRef]
18. Zheng, J.; Yu, T.; Lei, B.; Lv, R. Study on the influencing factors of thermal performance of radiant heating floor with the intensive solar irradiation. *Appl. Therm. Eng.* **2023**, *232*, 121077. [CrossRef]
19. Wang, Y.; Wu, X.; Gao, J.; Feng, A.; Wang, J.; Liu, D.; Zhou, X. Simplified model for heat transfer and surface temperature of prefabricated radiant heating and cooling system. *Energy Build.* **2022**, *276*, 112522. [CrossRef]
20. Yan Ren, Y.L.; Zhang, J.; Zhou, X.; Zhang, X. Calculation and engineering application of indoor comfort evaluation index of radiant air conditioning. *Build. Energy Environ.* **2020**, *39*, 12.
21. *Standard 138-2013*; Method of Testing for Rated Ceiling Panels for Sensible Heating and Cooling (ANSI Approved). ASHRAE: Peachtree Corners, GA, USA, 2013.
22. *EN-14240*; Ventilation for Buildings-Chilled Ceilings-Testing and Rating. European Committee for Standardization: Brussels, Belgium, 2004.

23. ASHRAE. *Handbook HVAC Systems and Equipment*; ASHRAE: Peachtree Corners, GA, USA, 2012.
24. Min, T.C.; Schutrum, L.; Parmelee, G.V. Natural Convection and radiation in a panel heated room. *ASHRAE Trans.* **1956**, *62*, 337–358.